Full Quantum Dynamics of Atom−Diatom Chemical Reactions in Hyperspherical Elliptic Coordinates†

Hideyuki Kamisaka,*,‡,§ Oleg I. Tolstikhin,||,⊥ and Hiroki Nakamura*,||

Department of Functional Molecular Science, School of Mathematical and Physical Science, The Graduate University for Advanced Studies, Myodaiji, Okazaki 444-8585, Japan, and Department of Theoretical Studies, Institute for Molecular Science, Myodaiji, Okazaki 444-8585, Japan

Received: February 28, 2004; In Final Form: April 10, 2004

Explicit expressions of the full Hamiltonian of tri-atomic system in the hyperspherical elliptic (HSE) coordinates are derived. The derivation is made from the expressions in the Delves coordinates. A numerical algorithm is also presented to evaluate the surface eigenfunctions including all the effects of Coriolis coupling terms. The whole formalism is numerically tested by using the Cl + DH and O(^{1}D) + HCl reaction systems. The HSE coordinate system, which is well-known to be powerful to elucidate reaction mechanisms especially for heavy−light−heavy systems, is now ready to be applied for clarifying full quantum dynamics of such systems.

1. Introduction

As is well-known, the hyperspherical coordinate approach is one of the most powerful methods to treat chemical reaction dynamics. This approach is useful not only for quantum dynamics but also for classical and semiclassical dynamics, as devised by Billing.[1,2] There are basically three types of hyperspherical coordinate systems for three-body systems, the Smith−Whitten type,[3−6] the Delves type,[7] and the hyperspherical elliptic (HSE) type.[8,9] These differ only in the definition of hyperangle variables. The HSE coordinate system is the most general one among them, because its definition apart from the overall orientation contains a free parameter.

A general theory of elliptic coordinate systems was developed by Jacobi.[10] Application of elliptic coordinates to hyperspherical studies of three-body systems was first discussed by Aquilanti et al.[11] However, these authors did not assume any relation between the parameter defining their coordinate system and the geometric characteristics of the physical system. In the HSE coordinates introduced independently by Tolstikhin et al.,[8] this parameter is fixed by the skew angle.[12] As a consequence, the HSE coordinate system is well adapted to the relief of the potential energy, which leads to approximate separability of the variables. The efficiency of this approach in applications to chemical reaction dynamics was demonstrated in refs 9, 13, and 14 (see also studies of three-body Coulomb systems).[8,15] Not only the high numerical efficiency is achieved but also chemical reaction dynamics can be nicely conceptualized as vibrationally nonadiabatic processes occurring in the vicinity of a potential ridge. This can be visualized as avoided crossings of the adiabatic potential energy curves as a function of hyperradius. Even analytical treatment of reaction dynamics can be carried out with use of the Zhu−Nakamura theory of nonadiabatic transition.[16−19] The HSE coordinates are especially convenient for studying chemical reactions with heavy−light−heavy (HLH) mass combination. In this case, with the help of good adiabaticity of the HSE hyperangles, we can further clarify the nonadiabatic reaction dynamics in the space of hyperangular variables and can project out the vibrationally adiabatic ridge lines onto the adiabatic potential-energy-curve diagram to elucidate reaction mechanisms.[20−22]

The actual applications of the HSE coordinates to chemical reactions have been limited only to J (total angular momentum quantum number) = 0. To make complete understanding of reaction dynamics in the HSE coordinate system possible, in this paper we formulate the full Hamiltonian in the HSE coordinates, including Coriolis coupling terms for nonzero J. At the same time an efficient numerical algorithm is proposed to carry out all the necessary numerical computations. The formulation and the algorithm are tested by applying to the Cl + HD reaction system. Some preliminary calculations for O(^{1}D) + HCl on the 2^1A′ PES are also carried out.

This paper is organized as follows. For later convenience, the definition of the HSE coordinates and some basic expressions in Delves coordinates are recalled in section II. In section III the kinetic energy operator expressed in terms of the HSE coordinates is derived with the help of the expressions given in section II. This is one of the main results of this paper. Section IV explains our numerical algorithm, especially about the preparation of basis functions to build up the surface eigenfunctions at fixed hyperradius and about the body-fixed (BF) frame transformation. The test calculations for the Cl + DH and O(^{1}D) + HCl reaction systems are reported in section V. Concluding remarks and possible future applications are discussed in section VI. Further detailed procedures of numerical calculations are explained in Appendix A, and Appendix B clarifies the definition of **S** matrix.

† Part of the "Gert D. Billing Memorial Issue".

* Authors to whom correspondence should be addressed. E-mail addresses: nakamura@ims.ac.jp, kami@tcl.t.u-tokyo.ac.jp.

‡ The Graduate University for Advanced Studies.

§ Present address: Department of Chemical System Engineering, School of Engineering, The University of Tokyo, 7-3-1 Hongo, Bunkyoku, Tokyo 113-8656, Japan.

|| Institute for Molecular Science.

⊥ Permanent address: Russian Research Center "Kurchatov Institute", Kurchatov Square 1, Moscow 123182, Russia.

10.1021/jp049102s CCC: $27.50
Published on Web 05/21/2004

2. Preliminaries

In this section, we provide the definition of our hyperspherical elliptic (HSE) coordinates, their relations to the Delves hyperspherical coordinates, and the kinetic energy operator expressed in terms of Delves coordinates. These will be used in later sections.

A. HSE Coordinates. The HSE coordinates consist of the usual hyperradius ρ and the following hyperangles (ξ_τ, η_τ):[9]

$$\rho = \sqrt{x_\tau^2 + y_\tau^2} \tag{1}$$

$$\xi_\tau = \chi_{\tau+1} + \chi_{\tau+2} \tag{2}$$

$$\eta_\tau = \chi_{\tau+1} - \chi_{\tau+2} \tag{3}$$

where χ_τ is one of the Delves hyperangles.[7] Hereafter we use the index τ to specify arrangement: $\tau = A$, for instance, designates the A + BC atom−diatom arrangement, and $\tau + 1$ and $\tau + 2$ are used to represent the other two arrangement channels. The Delves coordinates are defined in terms of the mass-scaled Jacobi coordinates x_τ and y_τ as[23]

$$\tan\frac{\chi_\tau}{2} = \frac{y_\tau}{x_\tau} \tag{4}$$

and

$$\cos\theta_\tau = \frac{\mathbf{x}_\tau \cdot \mathbf{y}_\tau}{x_\tau y_\tau} \tag{5}$$

with

$$\mathbf{x}_\tau = \sqrt{\frac{\mu_\tau}{\mu}}\,\mathbf{R}_\tau \tag{6}$$

and

$$\mathbf{y}_\tau = \sqrt{\frac{m_\tau}{\mu}}\,\mathbf{r}_\tau \tag{7}$$

where μ is the reduced mass of the system,

$$\mu = \sqrt{\frac{\bar{m}_\tau \bar{m}_{\tau+1} \bar{m}_{\tau+2}}{\bar{m}_\tau + \bar{m}_{\tau+1} + \bar{m}_{\tau+2}}} \tag{8}$$

$\bar{m}_\tau$ is the mass of the atom τ, μ_τ is the reduced mass in the arrangement τ, and m_τ is the reduced mass of diatomic molecule in the same arrangement. The Jacobi vector $\mathbf{R}_\tau$ is the vector pointing the atom τ from the center of mass of the diatomic molecule and the Jacobi vector $\mathbf{r}_\tau$ is the vector pointing $\tau + 2$ from $\tau + 1$.

B. Arrangement Transformation in Delves Coordinates. The transformation among different sets of Delves coordiantes ($\chi_{\tau+1}$, $\theta_{\tau+1}$) and ($\chi_{\tau+2}$, $\theta_{\tau+2}$) can be obtained by expressing the two sets of Smith−Whitten coordinates,[3,4] ($X_{\tau+1}$, $Y_{\tau+1}$, Z), ($X_{\tau+2}$, $Y_{\tau+2}$, Z), in terms of (ρ, $\chi_{\tau+1}$, $\theta_{\tau+1}$) and (ρ,$\chi_{\tau+2}$, $\theta_{\tau+2}$) and using Smith's kinematic rotation.[3,4] The result is as follows:[9]

$$\cos\chi_{\tau+2} = c_\tau \cos\chi_{\tau+1} + s_\tau \sin\chi_{\tau+1}\cos\theta_{\tau+1} \tag{9}$$

$$\sin\chi_{\tau+2}\cos\theta_{\tau+2} = -s_\tau \cos\chi_{\tau+1} + c_\tau \sin\chi_{\tau+1}\cos\theta_{\tau+1} \tag{10}$$

$$\sin\chi_{\tau+2}\sin\theta_{\tau+2} = \sin\chi_{\tau+1}\sin\theta_{\tau+1} \tag{11}$$

where

$$c_\tau = \cos 2\gamma_\tau \tag{12}$$

$$s_\tau = \sin 2\gamma_\tau \tag{13}$$

$$\tan\gamma_\tau = \sqrt{\frac{m_\tau(m_\tau + m_{\tau+1} + m_{\tau+2})}{m_{\tau+1}m_{\tau+2}}} \qquad 0 \le \gamma_\tau \le \frac{\pi}{2} \tag{14}$$

The angle γ_τ satisfies the following relation:

$$\gamma_\tau + \gamma_{\tau+1} + \gamma_{\tau+2} = \pi \tag{15}$$

From eqs 9, 10, and 15, we can obtain an important relation among χ_τ,

$$s_\tau \cos\chi_\tau + s_{\tau+1}\cos\chi_{\tau+1} + s_{\tau+2}\cos\chi_{\tau+2} = 0 \tag{16}$$

C. Kinetic Energy Operator in Delves Coordinates. Here, for later convenience, we recall the explicit expression of kinetic energy operator in Delves coordinates.[7,23,24] In the next section, the kinetic energy operator in HSE coordinates will be derived from this expression by using the coordinate transformations given above. Because, as is well-known, the body-fixed (BF) frame is more convenient than the space-fixed (SF) frame to describe reaction complex,[25] we use BF representation throughout this paper. Placing the BF z axis along the **y** vector, and putting the **x** vector in the xz plane ($x > 0$), we can express the kinetic energy operator T explicitly as

$$T \equiv T_\rho + T_{J=0} + T_{J>0} \tag{17}$$

with

$$2\mu T_\rho = -\hbar^2\left(\frac{\partial^2}{\partial\rho^2} + \frac{5}{\rho}\frac{\partial}{\partial\rho}\right) \tag{18}$$

$$2\mu T_{J=0} = -\frac{4\hbar^2}{\rho^2}\left(\frac{\partial^2}{\partial\chi^2} + \frac{2\cos\chi}{\sin\chi}\frac{\partial}{\partial\chi}\right) - \frac{4\hbar^2}{\rho^2\sin^2\chi}\left(\frac{\partial^2}{\partial\theta^2} + \frac{\cos\theta}{\sin\theta}\frac{\partial}{\partial\theta}\right) \tag{19}$$

and

$$2\mu T_{J>0} = \frac{4J_z^2}{\rho^2\sin^2\chi\sin^2\theta} + \frac{J(J+1) - 2J_z^2}{\rho^2\cos^2\frac{\chi}{2}} + \frac{1}{\rho^2\cos^2\frac{\chi}{2}} \times \left\{\frac{\cos\theta}{\sin\theta}(J_zJ_+ + J_zJ_-) + \hbar\frac{\partial}{\partial\theta}(J_- - J_+)\right\} \tag{20}$$

where J_+, J_-, J_z are the projections of the total angular momentum onto the BF frame.

The volume element is given by

$$\mathrm{d}^6\upsilon = \pi^2\rho^5\sin^2\chi\sin\theta\sin\beta\,\mathrm{d}\rho\,\mathrm{d}\chi\,\mathrm{d}\theta\,\mathrm{d}\alpha\,\mathrm{d}\beta\,\mathrm{d}\gamma \tag{21}$$

The present choice of BF frame is not unique, of course, and the other frames can be obtained by simple rotations (see

sections IV−B, for instance). Another convenient choice is, for instance, to take the *z* axis parallel to the **x** vector. In this case the corresponding kinetic energy operator can be obtained immediately by simple substitution of $\chi \rightarrow (\pi/2) - \chi$ in eq 4 and thus in eqs 19−20. This choice of BF frame has advantage in describing the asymptotic wave function.

3. Basic Equations in HSE Coordinates

In this section, we derive the kinetic energy operator in HSE coordinates by transforming the coordinates from the Delves. In principle, it is possible to use the rules of Podolsky[26] to achieve this. Unfortunately, however, the application of the Podolsky quantization rule has been found to be hopelessly complicated. We have found that the direct transformation of coordinates from Delves to HSE is much more convenient, although it is still complicated. Here, we outline this transformation procedure as concisely as possible.

A. Coordinate Transformation between HSE and Delves. Because the HSE angle variables (ξ_τ, η_τ) are defined in terms of $\chi_{\tau+1}$ and $\chi_{\tau+2}$ (see eqs 2 and 3), it is necessary to express χ_τ, θ_τ, $\theta_{\tau+1}$, and $\theta_{\tau+2}$ in terms of $\chi_{\tau+1}$ and $\chi_{\tau+2}$. χ_τ is easily evaluated from these two by using eq 16. Others, i.e., cos θ_τ, cos $\theta_{\tau+1}$, and cos $\theta_{\tau+2}$ can be expressed in terms of cos $\chi_{\tau+1}$ and cos $\chi_{\tau+2}$ as follows (see eqs 9 and 10)

$$\cos\theta_{\tau+1} = \frac{\cos\chi_{\tau+2} - c_\tau \cos\chi_{\tau+1}}{s_\tau \sin\chi_{\tau+1}} \tag{22}$$

$$\cos\theta_{\tau+2} = \frac{c_\tau \cos\chi_{\tau+2} - \cos\chi_{\tau+1}}{s_\tau \sin\chi_{\tau+2}} \tag{23}$$

and

$$\sin\chi_\tau \cos\theta_\tau = \frac{c_{\tau+2}\cos\chi_{\tau+2} - c_{\tau+1}\cos\chi_{\tau+1}}{s_\tau} \tag{24}$$

Because cos θ_τ always appears in the form of sin χ_τ cos θ_τ in the derivation, eq 24 is good enough.

The internuclear distances r_τ, $r_{\tau+1}$, and $r_{\tau+2}$ (r_τ designates the distance between the atoms $\tau + 1$ and $\tau + 2$, for instance) are easily obtained as[9]

$$r_\tau = \sqrt{\frac{1}{2m_\tau}}\left[1 + p_\tau^+ \cos\left(\frac{\xi_\tau}{2}\right)\cos\left(\frac{\eta_\tau}{2}\right) + p_\tau^- \sin\left(\frac{\xi_\tau}{2}\right)\sin\left(\frac{\eta_\tau}{2}\right)\right]^{1/2} \tag{25}$$

$$r_{\tau+1} = \sqrt{\frac{1}{m_\tau}}\sin\left(\frac{\xi_\tau + \eta_\tau}{4}\right) \tag{26}$$

and

$$r_{\tau+2} = \sqrt{\frac{1}{m_\tau}}\sin\left(\frac{\xi_\tau - \eta_\tau}{4}\right) \tag{27}$$

where p^+ and p^- are defined as

$$p^+ = \frac{s_2 + s_1}{s_3} = 1 + \frac{2m_3}{m_1 + m_2} \tag{28}$$

and

$$p^- = \frac{s_2 - s_1}{s_3} = \frac{m_1 - m_2}{m_1 + m_2} \tag{29}$$

B. Kinetic Energy Operator in HSE Coordinates. As mentioned before, we choose the BF-*z* axis to be parallel to the **y** vector with **x** in the *xz* plane ($x \geq 0$). Although the total wave function is naturally invariant for the choice of BF frame, the Coriolis coupling terms depend on the choice and numerical efficiency is affected. The HSE coordinate is convenient to describe the dynamics of heavy−light−heavy systems, whose internal momentum of inertia is close to that of a prolate top. In this case the projection of total angular momentum to the heavy−heavy axis (the axis of prolate top) approximately conserves; and thus it is appropriate to choose the **y** vector (heavy−heavy atom axis) as BF-*z* axis. In the following, we give the explicit expressions of $T_{J=0}$ and $T_{J>0}$ separately.

1. Expression of $T_{J=0}$. This part is independent of the arrangement τ. This can be easily understood from the fact that $T_{J=0}$ in the Smith−Whitten coordinates is invariant under Smith's kinematic rotation.[27] In the following we transform the $T_{J=0}$ in the Delves coordinates in the arrangement $\tau + 1$. Hereafter we omit τ for ξ and η so that (ξ, η) stands for (ξ_τ, η_τ). Similarly, χ_3, χ_1, and χ_2 (θ_3, θ_1, and θ_2) are used to designate χ_τ, $\chi_{\tau+1}$, and $\chi_{\tau+2}$ (θ_τ, $\theta_{\tau+1}$, and $\theta_{\tau+2}$), respectively.

Using the relations obtained from eq 9,

$$\left(\frac{\partial\chi_2}{\partial\chi_1}\right)_{\theta_1} = \frac{c_3 - \cos\chi_1\cos\chi_2}{\sin\chi_1\sin\chi_2} \tag{30}$$

and

$$\left(\frac{\partial\chi_2}{\partial\theta_1}\right)_{\chi^1} = \frac{s_3\sin\chi_1\sin\theta_1}{\sin\chi_2} = \frac{\sqrt{{s_3}^2\sin^2\chi_1 - (\cos\chi_2 - c_3\cos\chi_1)^2}}{\sin\chi_2} \tag{31}$$

we can obtain

$$\left(\frac{\partial}{\partial\chi_1}\right)_{\theta_1} = \left(\frac{\partial}{\partial\chi_1}\right)_{\chi_2} + \frac{c_3 - \cos\chi_1 - \cos\chi_2}{\sin\chi_1\sin\chi_2}\left(\frac{\partial}{\partial\chi_2}\right)_{\chi_1} \tag{32}$$

$$\left(\frac{\partial}{\partial\theta_1}\right)_{\chi_1} = \frac{\sqrt{{s_3}^2\sin^2\chi_1 - (\cos\chi_2 - c_3\cos\chi_1)^2}}{\sin\chi_2}\left(\frac{\partial}{\partial\chi_2}\right)_{\chi_1} \tag{33}$$

and

$$\frac{\cos\theta_1}{\sin\theta_1}\left(\frac{\partial}{\partial\theta_1}\right)_{\chi_1} = \frac{\cos\chi_2 - c_3\cos\chi_1}{\sin\chi_2}\left(\frac{\partial}{\partial\chi_2}\right)_{\chi_1} \tag{34}$$

Substituting these results into $T_{J=0}$, we obtain

$$2\mu T_{J=0} = -\frac{4\hbar^2}{\rho^2}\left\{\left(\frac{\partial^2}{\partial\chi_1^2}\right)_{\chi_2} + \left(\frac{\partial^2}{\partial\chi_2^2}\right)_{\chi_1} + \frac{2\cos\chi_1}{\sin\chi_1}\left(\frac{\partial}{\partial\chi_1}\right)_{\chi_2} + \frac{2\cos\chi_2}{\sin\chi_2}\left(\frac{\partial}{\partial\chi_2}\right)_{\chi_1} + \frac{2(c_3 - \cos\chi_1\cos\chi_2)}{\sin\chi_1\sin\chi_2}\frac{\partial^2}{\partial\chi_1\partial\chi_2}\right\} \quad (35)$$

Expressing χ_1 and χ_2 in terms of ξ and η, we can finally have[8]

$$2\mu T_{J=0} = -\frac{16\hbar^2}{\rho^2(\cos\eta - \cos\xi)} \times \left\{\left(\frac{\partial}{\partial\xi}\right)_\eta (c_3 - \cos\xi)\left(\frac{\partial}{\partial\xi}\right)_\eta + \left(\frac{\partial}{\partial\eta}\right)_\xi (\cos\eta - c_3)\left(\frac{\partial}{\partial\eta}\right)_\xi\right\} \quad (36)$$

2. Expression of $T_{J>0}$. With use of eqs 16 and 24 it can be shown that

$$\sin^2\frac{\chi_3}{2} = \frac{1}{2}\left(1 + \frac{s_2}{s_3}\cos\chi_2 + \frac{s_1}{s_3}\cos\chi_1\right) = \frac{1}{2}\left\{1 + p^+\cos\frac{\xi}{2}\cos\frac{\eta}{2} + p^-\sin\frac{\xi}{2}\sin\frac{\eta}{2}\right\} \quad (37)$$

$$\sin^2\chi_3\sin^2\theta_3 = \frac{s_3^2 - \cos^2\chi_2 - \cos^2\chi_1 + 2c_3\cos\chi_1\cos\chi_2}{s_3^2} = \frac{(c_3 - \cos\xi)(\cos\eta - c_3)}{s_3^2} \quad (38)$$

and

$$\frac{\cos\theta_3}{\sin\theta_3} = \frac{c_2\cos\chi_2 - c_1\cos\chi_1}{\sqrt{s_3^2 - \cos^2\chi_1 - \cos^2\chi_2 + 2c_3\cos\chi_1\cos\chi_2}} = \frac{(c_2 - c_1)\cos\frac{\xi}{2}\cos\frac{\eta}{2} - (c_2 + c_1)\sin\frac{\xi}{2}\sin\frac{\eta}{2}}{\sqrt{(c_3 - \cos\xi)(\cos\eta - c_3)}} \quad (39)$$

Using eqs 16, 24, and 11, the operator $\partial/\partial\theta_3$ can be transformed as

$$\left(\frac{\partial}{\partial\theta_3}\right)_{\chi_3} = s_2\sin\theta_1\left(\frac{\partial}{\partial\chi_1}\right)_{\chi_2} - s_1\sin\theta_2\left(\frac{\partial}{\partial\chi_2}\right)_{\chi_1} = \sqrt{(c_3 - \cos\xi)(\cos\eta - c_3)} \times \left\{\frac{s_2}{s_3\sin\chi_1}\left(\frac{\partial}{\partial\chi_1}\right)_{\chi_2} - \frac{s_1}{s_3\sin\chi_2}\left(\frac{\partial}{\partial\chi_2}\right)_{\chi_1}\right\}$$

$$= 2\frac{\sqrt{(c_3 - \cos\xi)(\cos\eta - c_3)}}{\cos\eta - \cos\xi} \times \left\{\left(p^-\sin\frac{\xi}{2}\cos\frac{\eta}{2} - p^+\cos\frac{\xi}{2}\sin\frac{\eta}{2}\right)\left(\frac{\partial}{\partial\xi}\right)_\eta + \left(p^+\sin\frac{\xi}{2}\cos\frac{\eta}{2} - p^-\cos\frac{\xi}{2}\sin\frac{\eta}{2}\right)\left(\frac{\partial}{\partial\eta}\right)_\xi\right\} \quad (40)$$

Substituting these results into eq 20, we finally obtain

$$2\mu T_{J>0} = \frac{4s_3^2 J_z^2}{\rho^2(c_3 - \cos\xi)(\cos\eta - c_3)} + \frac{J(J+1) - 2J_z^2}{\rho^2\left(1 + p^+\cos\frac{\xi}{2}\cos\frac{\eta}{2} + p^-\sin\frac{\xi}{2}\sin\frac{\eta}{2}\right)} + \frac{1}{\rho^2\left(1 + p^+\cos\frac{\xi}{2}\cos\frac{\eta}{2} + p^-\sin\frac{\xi}{2}\sin\frac{\eta}{2}\right)} \times \left[\frac{(c_2 - c_1)\cos\frac{\xi}{2}\cos\frac{\eta}{2} + (c_2 + c_1)\sin\frac{\xi}{2}\sin\frac{\eta}{2}}{\sqrt{(c_3 - \cos\xi)(\cos\eta - c_3)}} \times (J_zJ_+ + J_zJ_-) + \frac{2\hbar\sqrt{(c_3 - \cos\xi)(\cos\eta - c_3)}}{\cos\eta - \cos\xi} \times \left\{\left(p^-\sin\frac{\xi}{2}\cos\frac{\eta}{2} - p^+\cos\frac{\xi}{2}\sin\frac{\eta}{2}\right)\left(\frac{\partial}{\partial\xi}\right)_\eta + \left(p^+\sin\frac{\xi}{2}\cos\frac{\eta}{2} - p^-\cos\frac{\xi}{2}\sin\frac{\eta}{2}\right)\left(\frac{\partial}{\partial\eta}\right)_\xi\right\}(J_- - J_+)\right] \quad (41)$$

where

$$J_z = \frac{1}{\mathrm{i}}\frac{\partial}{\partial\gamma} \quad (42)$$

$$J_\pm = \mathrm{e}^{\pm\mathrm{i}\gamma}\left\{\cot\beta\left(\frac{1}{\mathrm{i}}\frac{\partial}{\partial\gamma}\right) - \frac{\partial}{\partial\beta} - \frac{1}{\sin\beta}\left(\frac{1}{\mathrm{i}}\frac{\partial}{\partial\alpha}\right)\right\} \quad (43)$$

The first and the second terms of eq 41 contain neither J_+ nor J_-. These terms represent the centrifugal barrier. The residual third term describes the Coriolis coupling.

The volume element in the HSE coordinates can be obtained easily from that of Delves coordinates. Starting from the volume element in the arrangement $\tau = 1$ (see eq 21) and using eq 22, we obtain

$$\sin^2\chi_1\sin\theta_1\,\mathrm{d}\theta_1\,\mathrm{d}\chi_1 = \frac{1}{s_3}\sin\chi_1\sin\chi_2\,\mathrm{d}\chi_1\,\mathrm{d}\chi_2 = \frac{1}{2s_3}(\cos\eta - \cos\xi)\,\mathrm{d}\chi_1\,\mathrm{d}\chi_2 \quad (44)$$

Thus we finally have

$$\mathrm{d}^6\upsilon = \frac{\pi^2}{4s_3}\rho^5(\cos\eta - \cos\xi)\sin\beta\,\mathrm{d}\rho\,\mathrm{d}\xi\,\mathrm{d}\eta\,\mathrm{d}\alpha\,\mathrm{d}\beta\,\mathrm{d}\gamma \quad (45)$$

4. Implementation of Numerical Procedures

In the scattering calculation, we solve the close-coupling equations along the hyperradius ρ, as usual. To do this, first we have to solve the surface eigenvalue problem at fixed ρ. In this section, our procedures are summarized for this surface eingenvalue problem.

A. Basis Functions—Inclusion of Coriolis Coupling. The surface eigenvalue problem is split into three steps and is solved by sequential diagonalization with use of new basis functions at each step. For convenience, the Delves hyperangles (χ_3, θ_3) are used occasionally, but their HSE representations can be easily obtained from eqs 37−40, if necessary. The actual

numerical integrations are, of course, carried out in the HSE coordinatates, and they are discussed in Appendix A.

First, we solve the eigenvalue problem for $T_{J=0}$ together with the first term of $T_{J>0}$ in the Ω representation and the electronic potential function. Hereafter we refer the solution of this equation as "primitive basis". This part requires relatively high computational efforts and is carried out for a selected set of hyperradius $\rho = \bar{\rho}$ and $\Omega = 0, 1, 2$. The equations to be solved are

$$\left[-\frac{8}{\rho^2(\cos\eta-\cos\xi)}\left\{\left(\frac{\partial}{\partial\xi}\right)_\eta(c_3-\cos\xi)\left(\frac{\partial}{\partial\xi}\right)_\eta+\left(\frac{\partial}{\partial\eta}\right)_\xi(\cos\eta-c_3)\left(\frac{\partial}{\partial\eta}\right)_\xi\right\}+\frac{2{s_3}^2\Omega^2}{(c_3-\cos\xi)(\cos\eta-c_3)}+\mu\rho^2(V(\xi,\eta;\bar{\rho})-\bar{U}_\nu^{J\Omega}(\bar{\rho}))\right]\bar{\Phi}_\nu^\Omega(\xi,\eta;\bar{\rho})=0 \quad (46)$$

For later convenience, the following two integrals are prepared (see eqs 20 and 58):

$$\bar{C}_{\nu'\nu}^{\Omega\Omega+1}=\left\langle\bar{\Phi}_{\nu'}^\Omega\left|\frac{1}{2\sin^2\frac{\chi_3}{2}}\frac{\cos\theta_3}{\sin\theta_3}\right|\bar{\Phi}_\nu^{\Omega+1}\right\rangle \quad (47)$$

and

$$\bar{C}'_{\nu'\nu}{}^{\Omega\Omega+1}=\left\langle\bar{\Phi}_{\nu'}^\Omega\left|\frac{1}{2\sin^2\frac{\chi_3}{2}}\frac{\partial}{\partial\theta_3}\right|\bar{\Phi}_\nu^{\Omega+1}\right\rangle \quad (48)$$

The calculation procedures of these quantities are given in Appendix A-4. Second, we solve the equation composed of $T_{J=0}$ and the centrifugal part of $T_{J>0}$ (see eqs 36 and 41) in the K representation,

$$\left[-\frac{8}{\rho^2(\cos\eta-\cos\xi)}\left\{\frac{\partial}{\partial\xi}(c_3-\cos\xi)\frac{\partial}{\partial\xi}+\frac{\partial}{\partial\eta}(\cos\eta-c_3)\frac{\partial}{\partial\eta}\right\}+\frac{2{s_3}^2K^2}{(c_3-\cos\xi)(\cos\eta-c_3)}+\frac{J(J+1)-2K^2}{2\left(1+p^+\cos\frac{\xi}{2}\cos\frac{\eta}{2}+p^-\sin\frac{\xi}{2}\sin\frac{\eta}{2}\right)}+\mu\rho^2(V(\xi,\eta;\rho)-\hat{U}_\lambda^{JK}(\rho))\right]\hat{\Phi}_\lambda^{JK}(\xi,\eta;\rho)=0 \quad (49)$$

by expanding in terms of the primitive basis:

$$\hat{\Phi}_\lambda^{JK}(\xi,\eta,\rho)=\sum_{\nu=1}^{N_{st}}C_\nu^{JK\lambda}\,\bar{\Phi}_\nu^\Omega(\xi,\eta;\bar{\rho}) \quad (50)$$

with

$$\Omega=\begin{Bmatrix}0 & K=0\\ 1 & K=1,3,5,\ldots\\ 2 & K=2,4,6,\ldots\end{Bmatrix} \quad (51)$$

The coefficients $C_\nu^{JK\lambda}$ are obtained from the following secular equation:

$$\sum_\nu(\delta_{\nu'\nu}\bar{U}_\nu^{J\Omega}+\bar{V}_{\nu'\nu}^{JK\Omega}(\rho,\bar{\rho}))C_\nu^{JK\lambda}=\hat{U}_\lambda^{JK}\,C_{\nu'}^{JK\lambda} \quad (52)$$

where

$$\bar{V}_{\nu'\nu}^{JK\Omega}(\rho,\bar{\rho})=\left\langle\bar{\Phi}_{\nu'}^\Omega(\chi,\theta,\bar{\rho})\left|\frac{2{s_3}^2(K^2-\Omega^2)}{(c_3-\cos\xi)(\cos\eta-c_3)}+\frac{J(J+1)-2K^2}{2\left(1+p^+\cos\frac{\xi}{2}\cos\frac{\eta}{2}+p^-\sin\frac{\xi}{2}\sin\frac{\eta}{2}\right)}+\mu(\rho^2V(\chi,\theta;\rho)-\bar{\rho}^2V(\chi,\theta;\bar{\rho}))\right|\bar{\Phi}_\nu^\Omega(\chi,\theta,\bar{\rho})\right\rangle \quad (53)$$

The selection of Ω for different K's as described above guarantees good convergence, because the behavior of wave function for odd and even K is different. Hereafter we refer these functions $\hat{\Phi}_\lambda^{JK}$ as "symmetric top basis". These are given for each set of ρ, J, and K.

Finally, we diagonalize the Coriolis coupling term by expanding the solution of surface function in terms of the symmetric top basis,

$$\Phi_\mu^{Jp}(\xi,\eta,\alpha,\beta,\gamma;\rho)=\sum_{K\lambda}C_{K\lambda}^{Jp\mu}\,\hat{\Phi}_\lambda^{JK}(\xi,\eta;\rho)\hat{\chi}_{MK}^{Jp}(\alpha,\beta,\gamma) \quad (54)$$

where

$$\hat{\chi}_{MK}^{Jp}(\alpha,\beta,\gamma)=\sqrt{\frac{2J+1}{16\pi^2(1+\delta_{K0})}}\times\{D_{-M-K}^J(\alpha,\beta,\gamma)+(-1)^{J+K+p}D_{-MK}^J(\alpha,\beta,\gamma)\} \quad (55)$$

Here we follow the definition of Wigner function given in ref 28 with p designating the parity of the total system:

$$p=\begin{Bmatrix}0 & \text{even parity}\\ 1 & \text{odd parity}\end{Bmatrix} \quad (56)$$

This symmetrized and normalized function $\hat{\chi}_{MK}^{Jp}$ describes the motion of the BF frame with definite total parity, total angular momentum, and its square of the BF-z projection. The following secular equation determines the coefficients $C_{K\lambda}^{Jp\mu}$:

$$\sum_{K\lambda}(\delta_{K'K}\delta_{\lambda'\lambda}\hat{U}_\lambda^{JK}+\delta_{K,K+1}\hat{C}_{\lambda'K\lambda K+1}^{Jp})C_{K\lambda}^{Jp\mu}=U_\mu^{Jp}(\rho)C_{K'\lambda'}^{Jp\mu} \quad (57)$$

where

$$\hat{C}^{Jp}_{\lambda' K \lambda K+1} = \begin{cases} -\sqrt{2J(J+1)} \times \left\langle \hat{\Phi}^{J0}_{\lambda'} \left| \frac{1}{2\sin^2\frac{\chi_3}{2}} \left(\frac{\cos\theta_3}{\sin\theta_3} + \frac{\partial}{\partial\theta_3} \right) \right| \hat{\Phi}^{J1}_{\lambda} \right\rangle & \text{for } K = 0 \text{ and } J+p \text{ is even} \\ -\sqrt{J(J+1) - K(K+1)} \times \left\langle \Phi^{JK}_{\lambda'} \left| \frac{1}{2\sin^2\frac{\chi_3}{2}} \left\{ (K+1)\frac{\cos\theta_3}{\sin\theta_3} + \frac{\partial}{\partial\theta_3} \right\} \right| \hat{\Phi}_{\lambda}{}^{JK+1} \right\rangle & \text{for } K > 0 \end{cases} \tag{58}$$

All the eigenvectors of secular equations are assumed to be normalized as $\sum_i |c_i|^2 = 1$.

B. BF Frame Transformation. So far we have used the BF frame with the *z* axis along the **y** vector. However, to represent the asymptotic wave functions, another choice of BF frame with BF-*z* axis along the **x** vector is more appropriate. When we designate the orientation of the former HSE BF frame as R^{e}, and that of the latter BF frame as R^{d} and the relative orientation of the latter from the former as R', the standard addition theorem for Wigner D function takes the form

$$D^J_{MM'}(R^{\mathrm{e}}) = \sum_{M''} D^J_{MM''}(R^{\mathrm{e}})\, D^J_{M''M'}(R') \tag{59}$$

Substituting this into eq 55, we obtain

$$\hat{\chi}^{Jp}_{MK}(R^{\mathrm{d}}) = \begin{cases} d^J_{00}(\theta)\, \hat{\chi}^{Jp}_{M0}(R^{\mathrm{e}}) + \sqrt{2}\sum_{K'=1}^{J} (-1)^{K'} d^J_{K'0}(\theta)\, \hat{\chi}^{Jp}_{MK'}(R^{\mathrm{e}}) & K = 0 \text{ and } J+p = \text{even} \\ (-1)^K \sqrt{2}\, d^J_{0-K}(\theta)\, \hat{\chi}^{Jp}_{M0}(R^{\mathrm{e}}) + (-1)^K \sum_{K'=1}^{J} \{ d^J_{-K'-K}(\theta) + (-1)^{J+K'+p} d^J_{K'-K}(\theta) \} \hat{\chi}^{Jp}_{MK'}(R^{\mathrm{e}}) & K > 0 \text{ and } J+p = \text{even} \\ (-1)^K \sum_{K'=1}^{J} \{ d^J_{-K'-K}(\theta) + (-1)^{J+K'+p} d^J_{K'-K}(\theta) \} \hat{\chi}^{Jp}_{MK'}(R^{\mathrm{e}}) & K > 0 \text{ and } J+p = \text{odd} \end{cases} \tag{60}$$

Definitions of the Euler angles and the Wigner *D* functions are taken from ref 28. Note that in this book, the rotated function $\psi'(x)$ is defined according to $\Psi(\mathbf{r}) \rightarrow \Psi(\mathbf{r}+\delta\mathbf{r})$ (equivalent to $\psi'(\mathbf{r}) = \psi(\mathbf{r}')$), where $\mathbf{r}'$ denotes the rotated position of $\mathbf{r}$. We have used more popular and intuitive definition $\psi'(\mathbf{r}') = \psi(\mathbf{r})$. The definition of θ for each Delves arrangement is depicted in Figure 1. This equation is of great use to transform the HSE wave function into that of Delves or Jacobi coordinates. Note that in eq 60 the BF frame is rotated whereas the physical system is fixed (passive rotation).

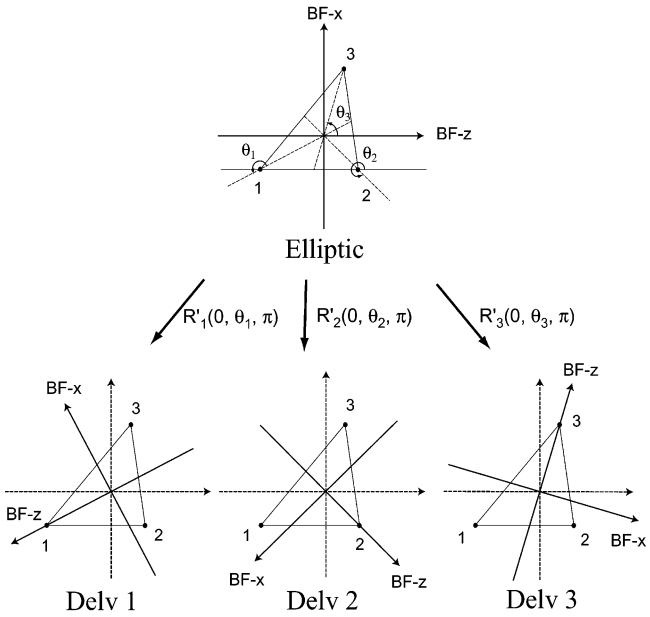

Figure 1. Definition of θ in the HSE-Delves BF frame transformation. The additional rotation R'_τ transforms the BF frame used in HSE into the one in Delves with arrangement τ. These rotations are depicted by Euler angles in middle of the figure. Note that these Euler angles are defined in terms of HSE BF frame.

TABLE 1: Number of DVR Basis Used in the Channel Functions of Cl + DH[a]

$\rho = 3.5-7.3\ a_0$ (HSE)		$\rho = 7.5-12.3\ a_0$ (Delves)			
			DCl	HCl	HD
N_ξ	130	N_χ	400(202)	400(144)	400(115)
N_η	130	N_θ	70	70	70
N_{ad}	30	N_{ad}	10	10	10
$N_{\mathrm{bas}}(\Omega=0)$	150	$N_{\mathrm{bas}}(\Omega=0)$	80	50	20
$N_{\mathrm{bas}}(\Omega=1)$	150	$N_{\mathrm{bas}}(\Omega=1)$	80	50	20
$N_{\mathrm{bas}}(\Omega=2)$	150	$N_{\mathrm{bas}}(\Omega=2)$	60	50	20
$N_{\mathrm{bas}}(\Omega=3)$	150	$N_{\mathrm{bas}}(\Omega=3)$	60	50	15
$N_{\mathrm{st}}(K=0)$	120	$N_{\mathrm{st}}(K=0)$	80	50	20
$N_{\mathrm{st}}(K=1)$	120	$N_{\mathrm{st}}(K=1)$	80	50	20
$N_{\mathrm{st}}(K=2)$	120	$N_{\mathrm{st}}(K=2)$	60	50	20
$N_{\mathrm{st}}(K=3)$	120	$N_{\mathrm{st}}(K=3)$	60	50	15
N_{ch}	300	N_{ch}	160	100	40

[a] The numbers in parentheses of N_χ indicate that only this number of the DVR basis around $\chi \sim 0$ is employed. The range of χ is restricted in each arrangement channel to solve each arrangement separately.

5. Numerical Examples

As a first example, we have studied the Cl + HD reaction on the BW4 potential energy surface (PES).[29] This reaction system is listed as one of the examples in the program ABC developed by Skouteris et al.[30] Their program has been used to successfully reproduce several experimental results.[31] Here we use their results as a reference.

The outline of the computational scheme is almost identical to our previous study.[9,32] First, we sectorize the hyperradius ρ which spans $3.5a_0-17.3a_0$ and is split into 69 sectors with the same interval $0.2a_0$. At the minimum ρ and the first 20 sector boundaries the primitive bases are prepared in the HSE coordinates. At other sector boundaries including the maximum ρ they are prepared in the Delves coordinates. The number of DVR basis[33] employed is listed in Table 1. Second, the basis functions are solved at the minimum and maximum ρ, each sector boundary, and 8 quadrature points within each sector. The quadrature points in the first sector are prepared by scaling the Jacobi polynomials $P^{(2,0)}(x)$. Other quadrature points are

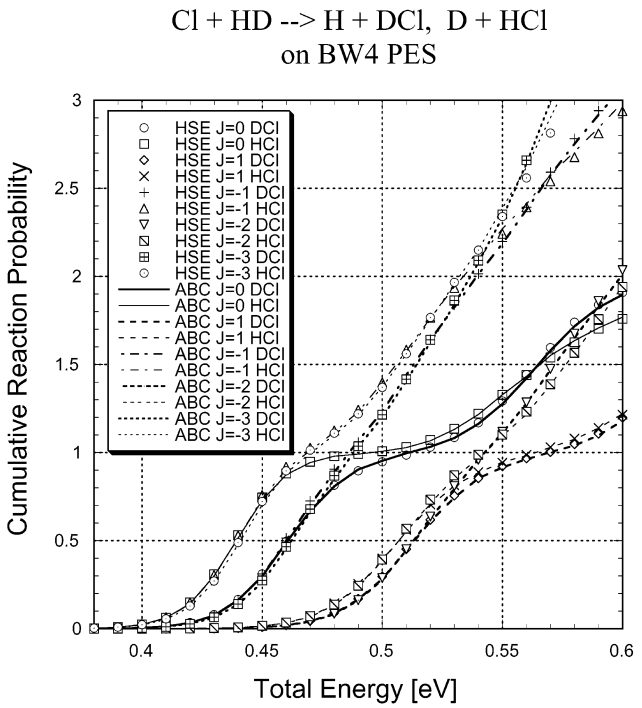

Figure 2. Total cumulative reaction probabilities for the Cl + HD reactions on BW4 PES. Thick lines represent the DCl production obtained by ABC. Thin lines represent the corresponding HCl production. The types of lines distinguish the total angular momentum. Various marks in the figure show the results of the present study.

TABLE 2: Number of Channels Used in the R Matrix Propagation of Cl + DH

	$J = 0$	$J = 1^+$	$J = 1^-$	$J = 2^-$	$J = 3^-$
N_{ch}	100	100	160	160	300

obtained by scaling the Legendre polynomials. Third, the **R** matrix propagation[34−38] is performed. This procedure is again quite similar to what we have used before.[9,32] The only extension is that the evaluation of overlap integrals between channel functions is now carried out for each quantum number K. This simply requires summation over K except for the HSE-Delves boundary, where eq 60 must be applied. In Table 2, the number of channel functions employed in the **R** matrix propagation is listed. Finally, the propagated **R** matrix is transformed into the **S** matrix by matching the channel functions to the asymptotic wave functions. To accelerate the convergence, the unperturbed asymptotic wave functions of spherical Bessel functions are used, and their derivatives with respect to ρ are evaluated with use of the chain rule.

Figure 2 shows the total cumulative reaction probabilities for $J = 0, 1^+, 1^-, 2^-, 3^-$ (the superscript designates the total parity of the system). We can see almost complete agreement. Figure 3 shows some of the state-to-state reaction probabilities for $J = 3^-$. In this figure, we used k instead of K to indicate that they are measured at the asymptotic limit. Here we can again confirm good agreement. The figure also indicates that for a collinearly constrained overbarrier type reaction only small number of K components contribute to the reaction. Figure 4 depicts the real and imaginary parts of state-to-state reaction amplitude. All these results guarantee that our present method and calculations are correct up to the detailed complex phases.

The total CPU time is found to be slightly longer than that of ABC in this reaction. This depends on the required accuracy, however, and the present results are supposed to be more

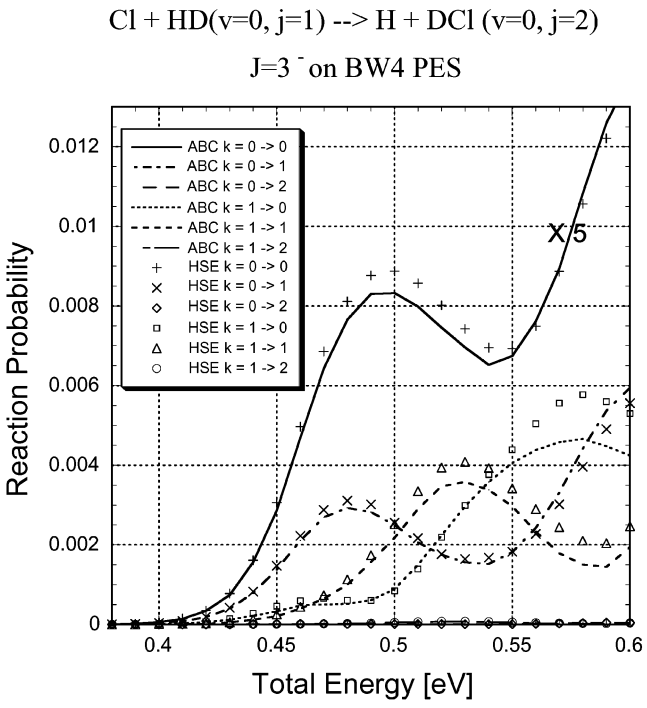

Figure 3. State-to-state reaction probabilities for Cl + HD(v=0,j=1) → H + DCl (v=0,j=2) on BW4 PES. The helicity quantum number k is also resolved and depicted separately in the figure. Various lines are the results of ABC, and the marks represent the corresponding results in the present calculation. The results for $k = 0 \rightarrow k' = 0$ are multiplied by the factor $^1/_5$.

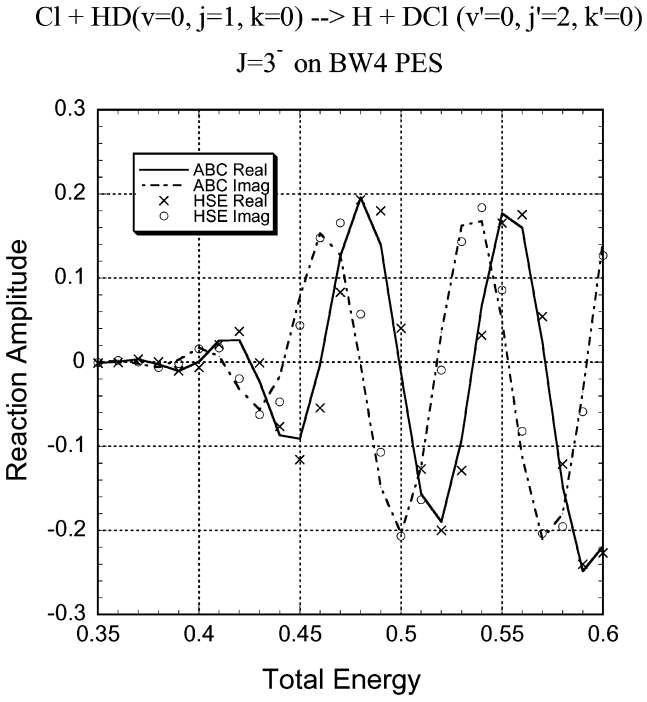

Figure 4. Real part and Imaginary part of the state-to-state reaction amplitude for Cl + HD(v=0,j=1,K=0) → H + DCl(v=0,j=2,K=0).

accurate. We have also studied O(^{1}D) + HCl on the 2^1A′ PES. The PES function is the same as what we have already reported before.[39−41] The range of ρ was chosen to be 5.20−20.12 au, sectoring 5.20−8.00 with 0.20 width, 8.00−15.92 with 0.18, and 15.92−20.12 with 0.20. The number of DVR basis, primitive basis, and symmetric top basis are listed in Table 3.

TABLE 3: Number of DVR Basis Used in the Channel Functions of O(^{1}D) + HCl[a]

$\rho = 5.2-9.98\ a_0$ (HSE)		$\rho = 10.16-15.56\ a_0$ (HSE)		$\rho = 15.74-20.12\ a_0$ (Delves)		
					HCl	OH
N_ξ	200(100)	N_ξ	200(100)	N_χ	800(143)	600(124)
N_η	120	N_η	120	N_θ	80	100
N_{ad}	45	N_{ad}	50	N_{ad}	15	25
N_{bas}	400	N_{bas}	400	N_{bas}	300	400
N_{st}	300	N_{st}	300	N_{st}	200	300
N_{ch}	700	N_{ch}	700	N_{ch}	700	700

[a] The range of ξ is restricted to reduce computational effort. Number of $N_{bas}(\Omega)$ and $N_{st}(K)$ is common for all $\Omega = 0$, 1, 2, 3 and $K = 0$, 1, 2, 3, respectiviely. N_{ch} in the list is for $J = 3^+$. See Table 4 for other J values.

TABLE 4: Number of Channels Used in the R Matrix Propagation of O(^{1}D) + HCl

	$J=0$	$J=1^+$	$J=1^-$	$J=2^-$	$J=2+$	$J=3^-$	$J=3^+$
N_{ch}	200	200	400	400	550	550	700

The number of channel function in the **R** matrix propagation is also listed in Table 4.

Figure 5 shows the total cumulative reaction probability of the system for several J. The total energy E_{tot} is measured from the potential bottom of HCl and the zero point energy of HCl is 0.19 eV.[40]

Figure 6 depicts the rovibrational distribution for one specific inital state, O(^{1}D) + HCl(v=0,j=14,k=2) for $J = 3^+$ at $E_{tot} =$ 0.544 eV. The overall reaction probability of this initial state is 0.658. Although the PES has the collinear transition state with OHCl configuration,[41] this result indicates that the initial state with $k = 2$ is also reactive. And the change of the k is not negligible. Thus, the conventional high K-component truncation and fixed K approximation (CS approximation) could be inapropriate in this system, and further detailed studies are necessary. The results show that the quantum numbers j and k are mostly conserved during the reaction. This conservation is supposed to be the adiabatic feature of the dynamics of HLH system, of which the motion of BF frame is close to that of prolate top. Hence, only the vibrationally nonadiabatic transition is expected to be playing the deterministic role. In the HSE coordinates the molecular vibration is closely correlated to the adiabatic ξ-motion, and accordingly, the vibrationally adiabatic ridge lines can be clearly defined. Chemical reactions can now be nicely conceptualized as vibrationally nonadiabatic transition in the vicinity of potential ridge lines.[9,13,14,22,39,40] Figure 6 actually shows the high selectivity of the reactive transitions as found before,[39,40] and this kind of selectivity can be nicely comprehended with use of the HSE channel functions.

6. Concluding Remarks

In this paper, we have presented the full formulation of quantum dynamics of triatomic reaction systems in terms of the hyperspherical elliptic coordinates. All terms of the total Hamiltonian including Coriolis couplings are treated exactly. Not only the complete mathematical formalism but also a numerical strategy to solve the resulting equations are explained. The entire numerical procedure is already implemented in our computer code. The correctness of the formulation and code is demonstrated by comparing the results with another existing code. This new methodology is expected to give all the scattering information with better numerical efficiency and physical understanding of reaction dynamics, especially for

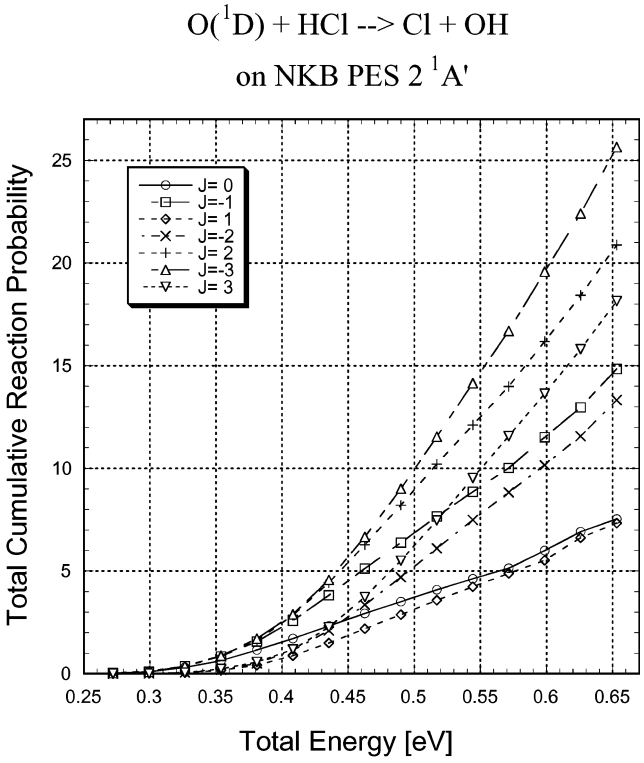

Figure 5. Total cumulative reaction probabilites for the O(^{1}D) + HCl reactions on 2^1A′ NKB PES.

systems with HLH mass combination. By using appropriate diabatic representation, we can easily employ the same methodology to investigate electronically nonadiabatic chemical reactions.[39,40] The quantum dynamics of O(^{1}D) + HCl, for instance, has been clarified on the basis of the accurate information of potential energy surfaces including the two excited ones.[39−41] This has been, however, limited only to $J =$ 0 with the three potential energy surfaces treated separately. With use of the present algorithm we can now clarify the full quantum dyanmics. We believe that the present method will add a new powerful tool to the hyperspherical coordinate approach to chemical reaction dynamics. Full applications to the O(^{1}D) + HCl system, for instance, will be reported in near future.

Acknowledgment. This research was supported in part by the Research Grant No.15002011 for Specially Promoted Project "Studies of Nonadiabatic Chemical Dynamics based on the Zhu-Nakamura theory" from the Ministry of Education, Culture, Sports, Science and Technology of Japan. O.I.T. thanks I. V. Komarov for drawing his attention to ref 10.

Appendix A. Details of Numerical Procedures

1. DVR Basis. The DVR basis is a popular technique for quantum molecular dynamics.[33] Here, we introduce the following DVR basis to deal with different boundary conditions of the Coriolis coupling terms. First, we introduce the following N functions $\varphi_n^{(m)}$:

$$\varphi_n^{(m)}(x) = (1-x^2)^m \tilde{\varphi}_n(x) \quad n = 1, ..., N,\ m = 0, {}^1/_2, 1 \quad \text{(A.1)}$$

$$\tilde{\varphi}_n(x) = \tilde{P}_{n-1}(x) \quad \text{(A.2)}$$

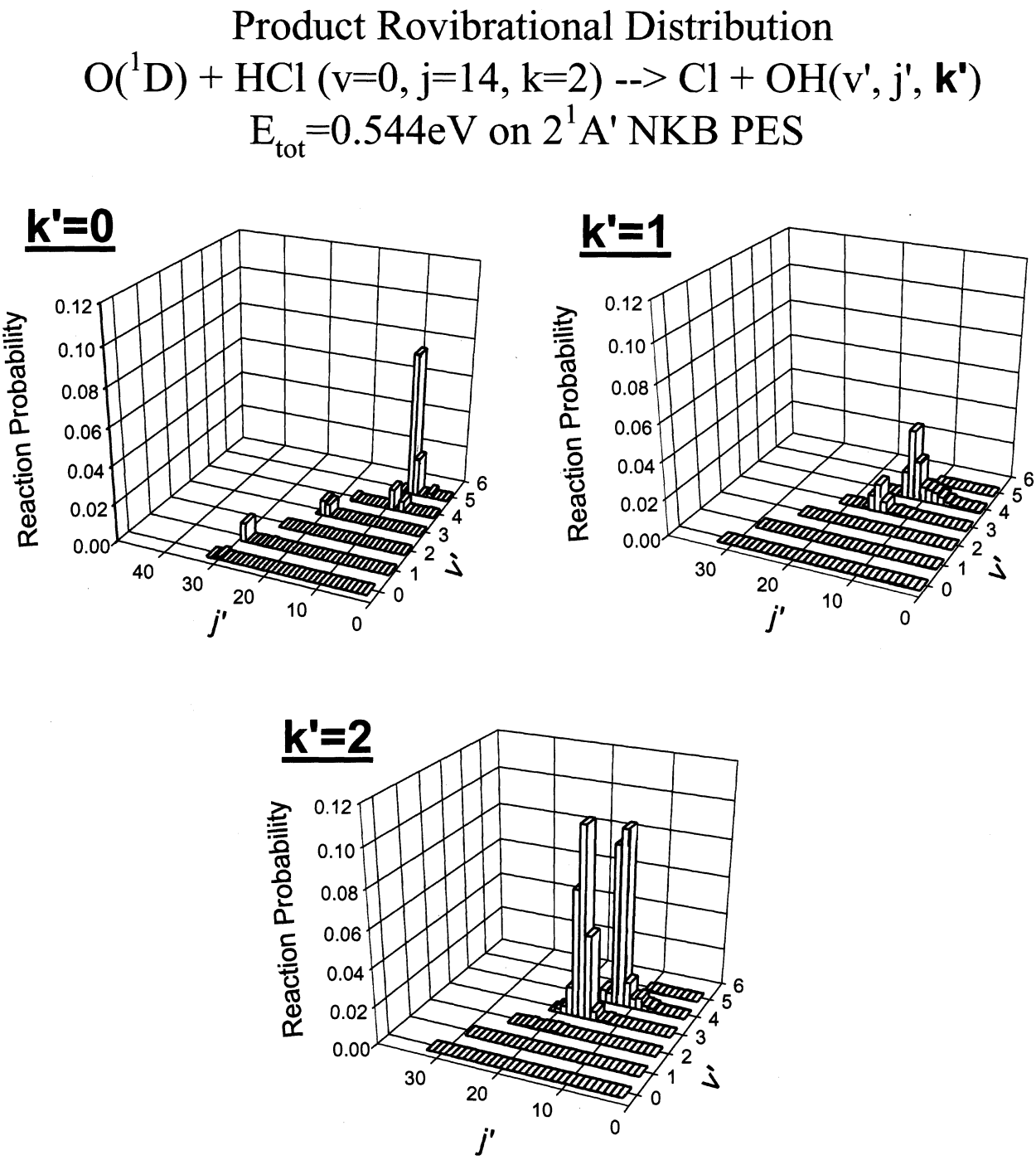

Figure 6. Product rovibrational distribution of for O(^{1}D) + HCl(v=0,j=14,k=2) $J = 3^+$ at $E_{tot} = 0.544$ eV.

where $\tilde{P}_{n-1}(x)$ is the normalized Legendre polynomial and the parameter m specifies the boundary behavior of the functions. The derivatives of these functions are given by

$$\varphi_n'^{(m)}(x) = (1 - x^2)^{m-1}\bar{\varphi}_n^{(m)} \tag{A.3}$$

with

$$\bar{\varphi}_n^{(m)}(x) = \frac{n(n+2m-1)}{\sqrt{(2n-1)(2n+1)}}\tilde{P}_n(x) + \frac{(n-1)(n-2m)}{\sqrt{(2n-3)(2n-1)}}\tilde{P}_{n-2}(x) \tag{A.4}$$

The functions $\bar{\varphi}_n^{(m)}(x)$ are introduced for later convenience.

Taking these $\varphi_n^{(m)}$ as basis, the DVR basis $\pi_i^{(m)}(x)$ can be constructed:

$$\pi_i^{(m)}(x) = \sum_{n=1}^{N} T_{ni}^{(m)}\varphi_n^{(m)}(x) \tag{A.5}$$

with

$$T_{ni}^{(m)} = \left(\frac{1}{1 - x_i^2}\right)^m T_{ni} \tag{A.6}$$

where T_{ni} is the standard DVR-FBR transformation matrix for Legendre polynomials. The pointwise character of these function is obvious from its definition and the nature of $\tilde{P}_{n-1}(x)$. Their orthogonality is guaranteed by the following approximate numerical integration:

$$\int_{-1}^{1}\pi_i^{(m)}(x)\,\pi_j^{(m)}(x)\,\mathrm{d}x \simeq \left(\frac{1}{1-x_i^2}\right)^m\left(\frac{1}{1-x_j^2}\right)^m\sum_{k=1}^{N}w_k\frac{\delta_{ik}}{\sqrt{w_i}}(1-x_k^2)^{2m}\frac{\delta_{jk}}{\sqrt{w_j}} \simeq \delta_{ij} \tag{A.7}$$

Here x_i and w_i are the standard Gauss−Legendre quadrature points and weights, respectively. Unlike the genuine DVR basis, the above orthogonality is not exact, but accurate for $m \ll N$. Because we only use $m = 0, {}^1/_2, 1$ in comparison with the number of quadrature points $N = 100-200$, the error is almost negligible. Thus the DVR basis $\pi_i^{(m)}(x)$ satisfies the two required conditions, adjustable boundary behavior and fixed quadrature points.

2. Integrals of Kinetic Energy Operator. We prepare two integrals of the kinetic energy operators in η and ξ space. Let us first consider the following integral:

$$\langle\pi_{i'}^{\eta}(\eta)|K_{\eta}|\pi_i^{\eta}(\eta)\rangle \tag{A.8}$$

where

$$\pi_i^{\eta}(\eta) = \frac{1}{\sqrt{2\gamma}}\,\pi_i^{(\Omega/2)}\left(\frac{\eta}{2\gamma}\right) \tag{A.9}$$

and

$$K_{\eta} = -8\left\{\frac{\partial}{\partial\eta}(\cos\eta - c)\frac{\partial}{\partial\eta} - \frac{s^2\Omega^2}{4(\cos\eta - c)}\right\} \tag{A.10}$$

Introducing $t = (\eta/2\gamma)$, we have

$$(\text{A.8}) = \frac{4}{\gamma^2}\int_{-1}^{1}\frac{\partial\pi_{i'}^{(\Omega/2)}(t)}{\partial t}\sin\gamma(1-t)\sin\gamma(1+t)\times \frac{\partial\pi_i^{(\Omega/2)}(t)}{\partial t}\,\mathrm{d}t + 2s^2\Omega^2\int_{-1}^{1}\pi_{i'}^{(\Omega/2)}(t)\times \frac{1}{\sin\gamma(1-t)\sin\gamma(1+t)}\,\pi_i^{(\Omega/2)}(t)\,\mathrm{d}t \tag{A.11}$$

In the case of $\Omega = 0$ this can be evaluated as

$$(\text{A.11}) = \sum_{k=1}^{N}\sum_{l=1}^{N}T_{ki'}T_{li}\frac{4}{\gamma^2}\int_{-1}^{1}(1-t^2)\varphi_k^{(0)}(t)\times \frac{\sin\gamma(1-t)\sin\gamma(1+t)}{(1-t)(1+t)}\varphi_l^{(0)}(t)\,\mathrm{d}t \tag{A.12}$$

Similarly, in the case of $\Omega > 0$ we have

$$(\text{A.11}) = \sum_{k=1}^{N}\sum_{t=1}^{N}\left(\frac{1}{1-x_{i'}^2}\right)^{\Omega/2}\left(\frac{1}{1-x_i^2}\right)^{\Omega/2}T_{ki'}T_{li}\times \int_{-1}^{1}(1-x^2)^{\Omega-1}\left\{\frac{4}{\gamma^2}\bar{\varphi}_k^{(\Omega/2)}(t)\frac{\sin\gamma(1-t)\sin\gamma(1+t)}{(1-t)(1+t)}\times \bar{\varphi}_t^{(\Omega/2)}(t) + s^2\Omega^2\bar{\varphi}_k(t)\frac{(1-t)(1+t)}{\sin\gamma(1-t)\sin\gamma(1+t)}\bar{\varphi}_l(t)\right\}\mathrm{d}t \tag{A.13}$$

Integrals eqs A.12 and A.13 can be computed with use of the Gauss−Gegenbaur quadrature accurately.[42]

Next, let us consider the following integral in ξ space:

$$\langle\pi_{i'}^{\xi}(\xi)|K_{\xi}|\pi_i^{\xi}(\xi)\rangle \tag{A.14}$$

where

$$\pi_i^{\xi}(\xi) = \frac{1}{\sqrt{\pi - 2\gamma}}\,\pi_i^{(\Omega/2)}\left(\frac{\xi - \pi}{\pi - 2\gamma}\right) \tag{A.15}$$

and

$$K_{\xi} = -8\left\{\frac{\partial}{\partial\xi}(c - \cos\xi)\frac{\partial}{\partial\xi} - \frac{s^2J_z^2}{4(c - \cos\xi)}\right\} \tag{A.16}$$

Using the new variable $t = (\xi - \pi)/(\pi - 2\gamma)$, it can easily be shown that eq A.16 is equivalent to eq 10 with $\gamma \rightarrow (\pi/2) - \gamma$.

3. Calculation of Primitive Basis. It can be easily seen that eq 46 has the separable form with respect to ξ and η (see the volume element given by eq 45):

$$\left[\frac{-8}{\cos\eta - \cos\xi}\left\{\frac{\partial}{\partial\xi}(c - \cos\xi)\frac{\partial}{\partial\xi} - \frac{s^2\Omega^2}{4(c - \cos\xi)} + \frac{\partial}{\partial\eta}(\cos\eta - c)\frac{\partial}{\partial\eta} - \frac{s^2\Omega^2}{4(\cos\eta - c)}\right\} + \nu\rho^2(V - U_{\nu})\right]\bar{\Phi}_{\nu} = 0 \tag{A.17}$$

This enables us to resort to the SDT technique[43−45] and solve the ξ and η motion sequentially. Assuming that we are dealing with heavy−light−heavy triatomic system, we solve the ξ motion first (For light−heavy−light system, η motion should be solved first, but this change is not substantial):

$$\left[\frac{-8}{\cos\eta_j - \cos\xi}\left\{\frac{\partial}{\partial\xi}(c - \cos\xi)\frac{\partial}{\partial\xi} - \frac{s^2\Omega^2}{4(c - \cos\xi)}\right\} + \mu\rho^2(V(\xi,\eta_j;\rho) - u_{n\xi}^j)\right]\phi_{n_{\xi}}(\xi;\eta_j,\rho) = 0 \tag{A.18}$$

The set of η_j is chosen to be the quadrature points of η. N_{ad} is the number of eigenfunctions of this η-fixed eigenvalue problem. Expanding the wave function in terms of the DVR basis functions introduced,

$$\phi_{n_{\xi}}(\xi,\eta_j;\rho) = \sum_{i=1}^{N_{\xi}}\frac{2\sqrt{s}}{\pi}\frac{c_i^{jn_{\xi}}\,\pi_i^{\xi}(\xi)}{\sqrt{(\cos\eta_j - \cos\xi_i)}} \tag{A.19}$$

and integrating the equation with use of the volume element

$(\pi^2/4s)(\cos\eta - \cos\xi)$, we obtain the following secular equation to determine the coefficient $c_i^{jn_\xi}$:

$$\sum_{i=1}^{N_\xi}\left[\frac{\langle\pi_{i'}^{\xi}|K_\xi|\pi_i^{\xi}\rangle}{\sqrt{(\cos\eta_j-\cos\xi_{i'})(\cos\eta_j-\cos\xi_i)}}+\mu\rho^2V(\xi_i,\eta_j,\rho)\delta_{i'i}\right]c_i^{jn_\xi}=\mu\rho^2u^j_{n_\xi}c_{i'}^{jn_\xi} \quad \text{(A.20)}$$

Subsequently, we expand the primitive basis in the following form:

$$\bar\Phi_\nu(\xi,\eta;\rho)=\sum_{n_\xi=1}^{N_{ad}}\sum_{j=1}^{N_\eta}c^\nu_{n_\xi j}\phi_{n_\xi}(\xi;\eta_j,\rho)\pi_j^\eta(\eta) \quad \text{(A.21)}$$

The coefficient $c^\nu_{n_\xi j}$ can be obtained by the following secular equation:

$$\sum_{n_\xi=1}^{N_{ad}}\sum_{j=1}^{N_\eta}[\langle\pi_{j'}^\eta(\eta)|K_\eta|\pi_j^\eta(\eta)\rangle O_{j'jn'_\xi n_\xi}+\mu\rho^2u^j_{n_\xi}\delta_{j'j}\delta_{n'_\xi n_\xi}]c^\nu_{n_\xi j}=\mu\rho^2U_\mu(\rho)c^\nu_{n'_\xi j'} \quad \text{(A.22)}$$

where

$$O_{j'jn'_\xi n_\xi}=\frac{\pi^2}{4s}\int_{2\gamma}^{2\pi-2\gamma}\phi_{n'_\xi}(\xi,\eta_{j'};\rho)\,\phi_{n_\xi}(\xi;\eta_j,\rho)\,d\xi=\sum_{i=1}^{N_\xi}\frac{c_i^{j'n'_\xi}c_i^{jn_\xi}}{\sqrt{(\cos\eta_{j'}-\cos\xi_i)(\cos\eta_j-\cos\xi_i)}} \quad \text{(A.23)}$$

Note that eqs A.22 and A.23 do not contain the volume element, because it has already been used in eq A.20. The eigenvectors $c_i^{jn_\xi}$ and $c^\nu_{n_\xi j}$ are assumed to be normalized as $\sum_i|c_i|^2=1$, as usual.

For the evaluation of Coriolis couplings, the basis functions $\bar\Phi_\nu^\Omega(\xi,\eta;\rho)$ have the separable form with respect to ξ and η and are expanded as follows:

$$\bar\Phi_\nu^\Omega(\xi,\eta;\rho)=\sum_{j=1}^{N_\eta}\sum_{i=1}^{N_\xi}\frac{2\sqrt{s}\,d_{ij}^{\Omega\nu}}{\pi\sqrt{\cos\eta_j-\cos\xi_i}}\pi_i^\xi(\xi)\pi_j^\eta(\eta) \quad \text{(A.24)}$$

From eqs A.19 and A.21 the coefficients $d_{ij}^{\Omega\nu}$ are defined by

$$d_{ij}^{\Omega\nu}=\sum_{n_\epsilon=1}^{N_{ad}}c^\nu_{n_\epsilon}c^{jn_\xi}c_i^{jn_\xi} \quad \text{(A.25)}$$

4. Calculation of Coriolis Couplings. Let us evaluate the Coriolis integral in eq 47,

$$\bar C^{\Omega\Omega+1}_{\nu'\nu}=\left\langle\bar\Psi^\Omega_{\nu'}\left|\frac{a(\xi,\eta)}{b(\xi,\eta)}\right|\bar\Psi^{\Omega+1}_\nu\right\rangle \quad \text{(A.26)}$$

where $a(\xi,\eta)$ and $b(\xi,\eta)$ are defined as follows (see eqs 37−39):

$$a(\xi,\eta)=\frac{(c_2-c_1)\cos\frac{\eta}{2}\cos\frac{\xi}{2}-(c_2+c_1)\sin\frac{\eta}{2}\sin\frac{\xi}{2}}{\sqrt{(c-\cos\xi)(\cos\eta-c)}} \quad \text{(A.27)}$$

and

$$b(\xi,\eta)=1+p^+\cos\frac{\eta}{2}\cos\frac{\xi}{2}+p^-\sin\frac{\eta}{2}\sin\frac{\xi}{2} \quad \text{(A.28)}$$

This integrand has singularity, and the numerical convergence is not guaranteed unless the singularity is handled properly. However, the wave function fortunately does not approach this point, because at this point two atoms $\tau+1$ and $\tau+2$ coalesce. Thus we can simply ignore this singularity and integrate the function with use of the same equadrature (ξ_i, η_j) as follows:

$$\text{(A.26)}=\sum_{i=1}^{N_\xi}\sum_{j=1}^{N_\eta}d_{ij}^{\Omega\nu'}\frac{a_{ij}}{b_{ij}}d_{ij}^{\Omega+1\nu} \quad \text{(A.29)}$$

where $a(\xi_i,\eta_j)$ and $b(\xi_i,\eta_j)$ are abbreviated to a_{ij} and b_{ij}.

Let us next consider the other integral in eq 48:

$$\bar C'_{\nu'\nu}{}^{\Omega\Omega+1}=\left\langle\bar\Phi^\Omega_{\nu'}\left|\frac{g(\xi,\eta)}{b(\xi,\eta)}\left(f^{(\xi)}(\xi,\eta)\frac{\partial}{\partial\xi}+f^{(\eta)}(\xi,\eta)\frac{\partial}{\partial\eta}\right)\right|\bar\Phi^{\Omega+1}_\nu\right\rangle \quad \text{(A.30)}$$

where $b(\xi,\eta)$ is defined by eq A.28 and $g(\xi,\eta)$, $f^{(\xi)}(\xi,\eta)$, and $f^{(\eta)}(\xi,\eta)$ are defined as

$$g(\xi,\eta)=\frac{2\sqrt{(c-\cos\xi)(\cos\eta-c)}}{\cos\eta-\cos\xi} \quad \text{(A.31)}$$

$$f^{(\xi)}(\xi,\eta)=p^-\sin\frac{\xi}{2}\cos\frac{\eta}{2}-p^+\cos\frac{\xi}{2}\sin\frac{\eta}{2} \quad \text{(A.32)}$$

and

$$f^{(\eta)}(\xi,\eta)=p^+\sin\frac{\xi}{2}\cos\frac{\eta}{2}-p^-\cos\frac{\xi}{2}\sin\frac{\eta}{2} \quad \text{(A.33)}$$

We need the ξ derivative and η derivative of $\bar\Phi_\nu^{\Omega+1}$ at (ξ_i,η_j). Noting that $\pi_j^\eta(\eta_j)=\delta_{j'j}(2\gamma w_j)^{-1/2}$, these can be evaluated as

$$\frac{d}{d\xi}\bar\Phi_\nu^{\Omega+1}(\xi_i,\eta_j)=\frac{2}{\pi}\sqrt{\frac{s}{2\gamma w_j}}\frac{1}{(\pi-2\gamma)^{3/2}}\times\sum_{n=1}^{N_\xi}\left(\sum_{i=1}^{N_\xi}\frac{d_{ij}^{\Omega+1\nu}}{\sqrt{\cos\eta_j-\cos\xi_i}}T_{ni}^{(m/2)}\right)\varphi_n'^{(m/2)}\left(\frac{\xi_i-\pi}{\pi-2\gamma}\right) \quad \text{(A.34)}$$

and

$$\frac{d}{d\eta}\bar\Phi_\nu^{\Omega+1}(\xi_i,\eta_j)=\frac{2}{\pi}\sqrt{\frac{s}{(\pi-2\gamma)w_i}}\frac{1}{(2\gamma)^{3/2}}\times\sum_{n=1}^{N_\eta}\left(\sum_{j=1}^{N_\eta}\frac{d_{ij}^{\Omega+1\nu}}{\sqrt{\cos\eta_j-\cos\xi_i}}T_{nj}^{(m/2)}\right)\varphi_n'^{(m/2)}\left(\frac{\eta_j}{2\gamma}\right) \quad \text{(A.35)}$$

Finally, eq A.30 is evaluated as follows:

$$\text{(A.30)}=\sum_{i=1}^{N_\xi}\sum_{j=1}^{N_\eta}\sqrt{w_iw_j}\,d_{ij}^{\Omega\nu'}\frac{g_{ij}}{b_{ij}}\left(f_{ij}^{(\xi)}\frac{d}{d\xi}\bar\Phi_\nu^{\Omega+1}(\xi_i,\eta_j)+f_{ij}^{(\eta)}\frac{d}{d\eta}\bar\Phi_\nu^{\Omega+1}(\xi_i,\eta_j)\right) \quad \text{(A.36)}$$

where w_i represents the weight factor of the ith Gauss−Legendre quadrature point out of N_ξ points and w_j is the weight for jth quadrature point out of N_η, respectively. The subscripts for g, $f^{(\xi)}$, and $f^{(\eta)}$ mean that these functions are evaluated at quadrature points (ξ_i, η_j).

Appendix B. Definition of S Matrix

We introduce the following wave function of noninteracting atom−diatom system:

$$\Psi^0_{jm} = \sqrt{\frac{\mu_\tau}{\hbar k_j}}\, \mathrm{e}^{\mathrm{i}k_j R\cos\theta_R} Y_{jm}(\theta_r,\phi_r) \tag{B.1}$$

with

$$k_j = \sqrt{2\mu_\tau(E_{\mathrm{tot}} - E_j)} \tag{B.2}$$

where μ_τ is the reduced mass of the atom−diatom system, E_j is the rotational energy of the diatomic molecule, and E_{tot} is the total energy of the system. The angles (θ_R, ϕ_R) and (θ_r, ϕ_r) are defined with respect to the SF frame. The normalization factor $\sqrt{(\mu_\tau/\hbar k_j)}$ is introduced so that the wave functions have unit probability flux density along R direction. Because we concern the definition of the **S** matrix here, we have ignored the vibrational motion of the diatomic molecule.

By rotating the xyz frame according to the Euler angle (ϕ_R, θ_R, 0), applying Rayleigh's formula[45] with $P_l(\cos\theta) = D^l_{00}(0,\theta,0)$, expanding the original spherical harmonics with those in new xyz frame, and finally using the addition theorem of Wigner functions and the symmetry properties of Clebsh−Gordan coefficients, the BF representation of eq B.1 is derived as[23]

$$(\mathrm{B.1}) = \sqrt{\frac{\mu_\tau}{\hbar k}} \sum_{J=|m|}^{\infty} (2J+1) \sum_{l=|J-j|}^{J+j} i^l j_l(kR) \sum_{m'=-\min(j,J)}^{\min(j,J)} (-1)^{m+m'} \times \langle jmJ - m|l0\rangle\langle jm'J - m|l0\rangle D^J_{-m-m'}(\phi_R,\theta_R,0)\, Y_{jm'}(\theta'_r,\phi'_r) \tag{B.3}$$

where (θ'_r, θ'_r) is the direction of diatomic molecule with respect to the BF frame (helicity representation).

Splitting the incoming and outgoing component, the wave function can be rewritten as

$$(\mathrm{B.1}) = \frac{\sqrt{\pi}}{k} \sum_{J=|m|}^{\infty} (2J+1)\{I^{JM}_{j-m} - O^{JM}_{jm}\} \tag{B.4}$$

where

$$I^{JM}_{j-m}(\mu_\tau,k,R) = \sqrt{\frac{\mu_\tau k}{\pi\hbar}} \sum_{K=-j}^{j} D^J_{-M-K}(\phi_R,\theta_R,0)\, Y_{jK}(\theta'_r,\phi'_r) \times \sum_{l=|J-j|}^{J+j} i^l \frac{h^{(2)}_l(kR)}{2} \langle jmJ - m|l0\rangle\langle jKJ - K|l0\rangle \tag{B.5}$$

and

$$O^{JM}_{jm}(\mu_\tau,k,R) = -\sqrt{\frac{\mu_\tau k}{\pi\hbar}} \sum_{K=-j}^{j} D^J_{-M-K}(\phi_R,\theta_R,0)\, Y_{jK}(\theta'_r,\phi'_r) \times \sum_{l=|J-j|}^{J+j} i^l \frac{h^{(1)}_l(kR)}{2} \langle jmJ - m|l0\rangle\langle jKJ - K|l0\rangle \tag{B.6}$$

The superscript M is equal to m, but we used M to indicate that this represents the z component of the total angular momentum. The subscripts of I^{JM}_{j-m} and O^{JM}_{jm} represent their asymptotic helicity quantum numbers:

$$I^{JM}_{j-m}(\mu_\tau,k,R) \xrightarrow{R\to\infty} \sqrt{\frac{\mu_\tau k}{\pi\hbar}}\, i^{J+j+1} D^J_{-Mm}(\phi_R,\theta_R,0)\, Y_{j-m}(\theta'_r,\phi'_r) \times \frac{\mathrm{e}^{-\mathrm{i}\{kR-(J+j)\pi/2\}}}{2kR} \tag{B.7}$$

and

$$O^{JM}_{jm}(\mu_\tau,k,R) \xrightarrow{R\to\infty} \frac{\mu_\tau k}{\pi\hbar}\, i^{J+j+1} D^J_{-M-m}(\phi_R,\theta_R,0)\, Y_{jm}(\theta'_r,\phi'_r) \times \frac{\mathrm{e}^{\mathrm{i}\{kR-(J+j)\pi/2\}}}{2kR} \tag{B.8}$$

The different signs of m in I^{JM}_{j-m} and O^{JM}_{jm} reflect the flipping of the BF frame that occurs even in the noninteracting atom−diatom system.[23] Note that the probability flux densities of these two functions are normalized as unity when integrated over the entire solid angle. These equation also indicate that $m = K$ at asymptotic limit.

The **S** matrix is defined according to the asymptotic behavior of the perturbed wave function as

$$\Psi_{jm} \to \frac{\sqrt{\pi}}{k_j} \sum_{J=|m|}^{\infty} (2J+1)\{I^{JM}_{j-m}(\mu_\tau,k_j,R) - \sum_{j'm'} S^J_{j'm'j-m}\, O^{JM}_{j'm'}(\mu_\tau,k_{j'},R)\} \tag{B.9}$$

Because of the invariance of the Hamiltonian under the parity operation $r \to -r$ and $R \to -R$, we can further decompose the entire problem. Using the total parity of the system given by $j + l$, let us introduce the parity-adapted incoming and outgoing components as follows:

$$\begin{Bmatrix} I^{JMp}_{jm} \\ O^{JMp}_{jm} \end{Bmatrix} = \begin{Bmatrix} I^{JM}_{jm} \\ O^{JM}_{jm} \end{Bmatrix}$$

with substitution

$$\sum_{l=|J-j|}^{J+j} \to \frac{1}{\sqrt{1+\delta_{m0}}} \sum_{l=|J-j|}^{J+j} \delta_{j+l,p} \tag{B.10}$$

The factor $1/\sqrt{1+\delta_{m0}}$ is introduced to normalize the probability flux density. The parity-adapted **S** matrix can be defined for each fixed J and p as

$$\Psi^{Jp}_{jm} \to C\{I^{JMp}_{jm} - \sum_{j'm'} S^{Jp}_{j'm'jm}\, O^{JMp}_{j'm'}\} \quad (m \ge 0,\, m' \ge 0) \tag{B.11}$$

where C is an arbitrary constant. Due to the symmetry of I_{jm}^{JMp} and O_{jm}^{JMp} with respect to m,

$$I_{jm}^{JMp} = (-1)^{J+p} I_{j-m}^{JMp} \tag{B.12}$$

$$O_{jm}^{JMp} = (-1)^{J+p} O_{j-m}^{JMp} \tag{B.13}$$

the original **S** matrix can be obtained from this parity-adapted **S** matrix as

$$S_{j'm'jm}^{J} = S_{j'-m'j-m}^{J} = \frac{\sqrt{(1+\delta_{m0})(1+\delta_{m'0})}}{2}(S_{j'm'jm}^{J+} + S_{j'm'jm}^{J-}) \tag{B.14}$$

and

$$S_{j'-m'jm}^{J} = S_{j'm'j-m}^{J} = (-1)^{J}\frac{\sqrt{(1+\delta_{m0})(1+\delta_{m'0})}}{2}(S_{j'm'jm}^{J+} - S_{j'm'jm}^{J-}) \tag{B.15}$$

This definition of the parity-adapted **S** matrix is the same as that of ABC.[30]

References and Notes

(1) Billing, G. D.; Balakrishnan, N.; Markovic, N. Application of Semiclassical Dynamics to Chemical Reactions. In *Dynamics of Molecular and Chemical Reactions*; Wyatt, R. E., Zhang, J. Z. H., Eds.; Marcel Dekker: New York, 1996.

(2) Adhikari, S.; Billing, G. D. *Chem. Phys.* **1998**, *238*, 69.

(3) Smith, F. T. *J. Math. Phys.* **1962**, *3*, 735.

(4) Whitten, R. C.; Smith, F. T. *J. Math. Phys.* **1968**, *9*, 1103.

(5) Johnson, B. R. *J. Chem. Phys.* **1980**, *73*, 5051.

(6) Kupperman, A. *Chem. Phys. Lett.* **1975**, *32*, 374.

(7) Delves, L. M. *Nucl. Phys.* **1958**/**1959**, *9*, 391; **1960**, *20*, 275.

(8) Tosltikhin, O. I.; Watanabe, S.; Matsuzawa, M. *Phys. Rev. Lett.* **1995**, *74*, 9573.

(9) Tolstikhin, O. I.; Nakamura, H. *J. Chem. Phys.* **1998**, *108*, 8899.

(10) Jacobi, C. G. J. *J. Reine Angew. Math.* **1839**, *19*, 309. See also: Jacobi, C. G. J. *Vorlesungen über Dynamics*; Druck und Verlang von G. Reimer: Berlin, 1884; Lecture 26.

(11) Aquilanti, V.; Cavalli, S.; Grossi, G. *J. Chem. Phys.* **1986**, *85*, 1362.

(12) A relation between elliptic coordinates considered in ref 11 and the HSE coordinate system introduced in ref 8 has recently been discussed by: Aquilanti, V.; Tonzani, S. *J. Chem. Phys.* **2004**, *120*, 4066.

(13) Nobusada, K.; Tolstikhin, O. I.; Nakamura, H. *J. Chem. Phys.* **1998**, *108*, 8922.

(14) Mil'nikov, G. V.; Tolstikhin, O.I.; Nobusada, K.; Nakamura, H. *Phys. Chem. Chem. Phys.* **1999**, *1*, 1159.

(15) Tolstikhin, O. I.; Matsuzawa, M. *Phy. Rev. A* **2001**, 062705.

(16) Zhu, C.; Nakamura, H.; Nobusada, K. *Phys. Chem. Chem. Phys.* **2000**, *2*, 557.

(17) Zhu, C.; Teranishi, Y.; Nakamura, H. *Adv. Chem. Phys.* **2001**, *117*, 127.

(18) Zhu, C.; Mil'nikov, G. V.; Nakamura, H. In *Modern Trends in Chemical Reactions and Dynamics*; Liu, K., Yang, X., Eds.; World Scientific: Singapore, 2004.

(19) Nakamura, H. *Nonadiabatic Transition: Concepts, Basic Theories and Applications*; World Scientific: Singapore, 2002.

(20) Nobusada, K.; Tolstikhin, O. I.; Nakamura, H. *J. Phys. Chem. A* **1998**, *102*, 9445.

(21) Nobusada, K.; Tolstikhin, O. I.; Nakamura, H. *J. Mol. Struct. Theor. Chem.* **1999**, *461*−*1*, 137.

(22) Nobusada, K.; Nakamura, H.; Lin, Y. J.; Ramachandran, B. *J. Chem. Phys.* **2000**, *113*, 1018.

(23) Schatz, G. C.; Kupperman, A. *J. Chem. Phys.* **1975**, *65*, 4642.

(24) Pack, R. T.; Parker, G. A. *J. Chem. Phys.* **1987**, *87*, 3888.

(25) Pack, R. T. *J. Chem. Phys.* **1973**, *60*, 633.

(26) Podolsky, B. *Phys. Rev.* **1928**, *32*, 812.

(27) Johnson, B. R. *J. Chem. Phys.* **1983**, *79*, 1906 and 1911.

(28) Varshalovich, D. A.; Moskalev, A. N.; Khersonskii, V. K. *Quantum Theory of Angular Momentum*; World Scientific: Singapore, 1988.

(29) Bian, W.; Werner, H-J. *J. Chem. Phys.* **2000**, *112*, 220.

(30) Skouteris, D.; Castillo, J. F.; Manolopoulos, D. E. *Comput. Phys. Commun.* **2000**, *133*, 123.

(31) Skouteris, D.; Werner, H- J.; Aoiz, F. J.; Banares, L.; Castillo, J. F.; Menendez, N.; Balucani, N.; Cartechini, N.; Casavecchia, P. *J. Chem. Phys.* **2001**, *114*, 10662.

(32) Kamisaka, H.; Bian, W.; Nobusada, K.; Nakamura, H. *J. Chem. Phys.* **2002**, *116*, 654.

(33) Light, J. C.; Hamilton, I. P.; Lill, J. V. *J. Chem. Phys.* **1985**, *82*, 1400.

(34) Bloch, C. *Nucl. Phys.* **1957**, *4*, 503.

(35) Lane, A. M.; Robson, D. *Phys. Rev.* **1966**, *151*, 774.

(36) Light, J. C.; Walker, R. B. *J. Chem. Phys.* **1976**, *65*, 4272.

(37) Stechel, E. B.; Walker, R. B.; Light, J. C. *J. Chem. Phys.* **1978**, *69*, 3518.

(38) Baluja, K. L.; Burke, P. G.; Morgan, L. A. *Comput. Phys. Commun.* **1982**, *27*, 299.

(39) Kamisaka, H.; Nakamura, H.; Nanbu, S.; Aoyagi, M.; Bian, W.; Tanaka, K. *J. Theor. Comput. Chem.* **2002**, *1*, 275.

(40) Kamisaka, H.; Nakamura, H.; Nanbu, S.; Aoyagi, M.; Bian, W.; Tanaka, K. *J. Theor. Comput. Chem.* **2002**, *1*, 285.

(41) Nanbu, S.; Aoyagi, M.; Nakamura, H.; Kamisaka, H.; Bian, W.; Tanaka, K. *J. Theor. Comput. Chem.* **2002**, *1*, 263.

(42) Press, W. H.; Teakolsky, S. A.; Vetterling, W. T.; Flannery, B. P. *Numerical Recipes in FORTRAN*; Cambridge University: Cambridge, 1992.

(43) Light, J. C.; Bačić, Z. *J. Chem. Phys.* **1987**, *87*, 4008.

(44) Mil'nikov, G. V.; Nakamura, H. *Comput. Phys. Commun.* **2001**, *140*, 381.

(45) Abramowitz, M.; Stegun, I. A. *Handbook of Mathematical Functions*; Dover: New York, 1972.